



# Transmission of pacemaker signal in a small world neuronal networks: temperature effects

Zhiwei He · Chenggui Yao · Shuai Liu · Yu Qian

Received: 19 May 2021 / Accepted: 10 September 2021 / Published online: 18 October 2021  
© The Author(s), under exclusive licence to Springer Nature B.V. 2021

**Abstract** The environmental temperature plays a crucial role in determining the behavior of any dynamical system. In particular, living organisms are characterized by a specific value of temperature, which ensures their normal functioning. In this paper, the effect of temperature on signal transmission of a pacemaker neuron is investigated using a small-world neuronal networks in which the pacemaker is stimulated by a square-wave signal. We observe that signal propagation may be significantly enhanced at intermediate temperatures, i.e., temperature favors the propagation of the rhythm of the pacemaker to the whole neuronal network. Furthermore, a rich dynamics is observed, including spiking and bursting activities, as well as full and remote synchronization. We also find that signal propagation crucially depends on the strength of the coupling. Our findings provide new insights on the system dynamics, and improve our understanding of the

optimal temperature observed in experiments involving living biological systems.

**Keywords** Neurodynamics · Signal transmission · Temperature · Small world · Electrical synapse

## 1 Introduction

The rhythmicity of some human behaviors, including walking, eating emanate, and breathing, depends on pacemaker neurons which are solitary neurons in the neuronal networks that entrain the behavior of other neurons to a coherent rhythmic activity [1]. Pacemaker neurons can guide the rhythmic activities of neighboring neurons, and stabilize the functioning of the whole networks. Due to the significance of pacemaker, much attention has been devoted to discuss the effects of pacemaker on the central pattern generator of neuronal system [2–7]. For example, rhythmic activities driven by a pacemaker ensemble may be observed in the central pattern generator of pyloric of *Panulirus interruptus*: these pacemakers are composed of an anterior buster and two pyloric dilator neurons [8]. Besides, the spontaneous circulating waves of activity controlled by the pacemakers embedded in a conducting medium have been observed in excitable media [9].

To investigate theoretically the rhythmic behavior, computational simulations of neuronal networks are usually employed [10–13]. In models of neuronal network, the complex behavior is determined by the

---

Z. He  
Department of Mathematics, Shaoxing University,  
Shaoxing, China

C. Yao (✉)  
College of Data science, Jiaying University, Jiaying  
314000, China  
e-mail: yaochenggui2006@126.com

S. Liu  
College of Science, Northwest A & F University, Yangling  
712100, China

Y. Qian  
Nonlinear Research Institute, Baoji University of Arts and Sciences,  
Baoji 721007, China

dynamics of the node and by the interactions between neurons [14–21]. It is noteworthy that these models are not only powerful to investigate the neurodynamics, but also an effective tool to discuss problems in physical, biological, chemical and ecological systems. Generally speaking, the complexity of neuronal activities is largely determined by the topological structure of the network. It is well-known that different structure leads to different dynamical behaviors. In connection-based schemes of brain network, the structure commonly exhibits small-world property [22,23]. Small-world (SW) networks have been proposed by Watts and Strogatz to understand the nature of real networks due to the faultiness of regular or random networks on revealing the dynamics of the real-life network [24]. Since then, the applications of small-world networks in nervous system greatly contribute to understand the complex dynamics of neurons, and have attracted large interest [25–33].

In nature, the microenvironment of a system has a significant effect on the complex behavior of coupled neurons. For example, the extracellular potassium concentrations [34–39], cell volume [40,41], and oxygen concentration [42–44], play a crucial role in the electrical brain activity which has a close relationship with neurological diseases, including epilepsy, Parkinson and arrhythmias. In this framework, temperature is an important environmental factor, and critically determines whether the physiological function of living organisms works normally. It is common knowledge that the most effective function of any biological system can only occur at an appropriate temperature or in a narrow range. For example, the comfortable temperature for the normal human body is about 18°–25°C. Many experiments reveal the importance of temperature on biological organisms [45–47]. Recently, theoretical models have revealed the important effects of temperature on the transmission of action potentials along axons, and the existence of an optimal temperature for action-potential propagation through myelinated axons [48]. The existence of an optimal temperature for biological organisms is also revealed by the fact that the maximum efficiency of system functioning may be often maintained only at a given temperature [49–53].

In this paper, we study the effect of temperature on the rhythmic behavior of neuronal networks with small-world topology driven by a pacemaker. In particular, we consider one neuron stimulated by a square wave sig-

nal as the pacemaker and analyze the dynamics of the system. Our findings reveal that the signal of the pacemaker may be transmitted to the whole neuronal network at an appropriate temperature. Additionally, the coupling strength plays a similar role in signal transmission of pacemaker. In particular, the response of the neuronal network depends nonmonotonically on the coupling strength, indicating that a resonance behavior occurs. Furthermore, we observe a rich dynamical behavior, including spiking and bursting activities, full synchronization and remote synchronization. The paper is structured as follows. In Sect. 2, the small-world neuronal network with Hodgkin–Huxley model is introduced, and a figure of merit to quantify signal transmission is presented. Some interesting results are shown in Sect. 3. Section 4 closes the paper with some concluding remarks.

### 2 Models and methods

In order to investigate the effect of temperature on the signal transmission of pacemaker in a small world neuronal networks, we employ the coupled Hodgkin–Huxley neuron model [48,53],

$$\begin{aligned}
 C_m \frac{dV_i}{dt} = & -(g_K n_i (V_i - V_K) \\
 & + g_{Na} m_i^3 h_i (V_i - V_{Na}) + g_l (V_i - V_l)) \\
 & + I_{i=d} \times i_0(t) + \frac{\epsilon}{k_i} \sum_{j=1}^N g_{i,j} (V_j - V_i), \quad i=1, \dots, N,
 \end{aligned}
 \tag{1}$$

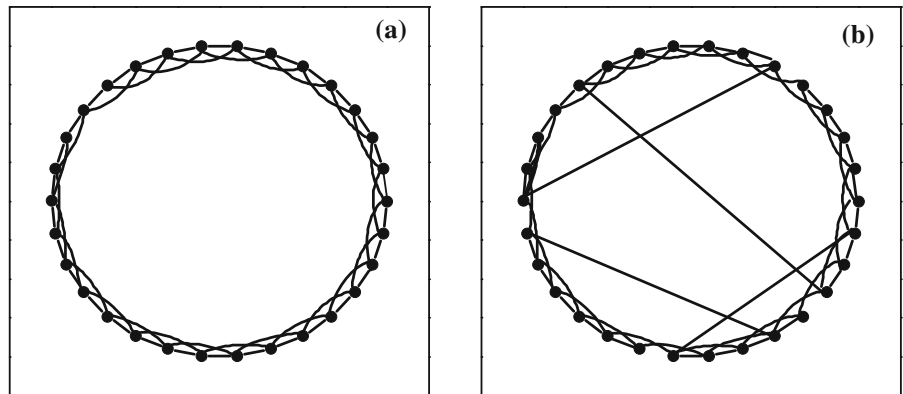
where  $V_i$  stands for the membrane potential, the sodium current is regulated by the gating variables for activation and inactivation which are denoted by  $m_i$  and  $h_i$ , respectively, and  $n_i$  is the activation gating variable for the potassium current. These gating variables can be written unanimously as,

$$\frac{dx_i}{dt} = \frac{1}{\tau_{x_i}} (-x_i + x_i^\infty), \quad x_i = m_i, n_i, h_i, \tag{2}$$

where  $\tau_{x_i} = \frac{1}{\alpha_{x_i} + \beta_{x_i}}$ , and  $x_i^\infty = \frac{\alpha_{x_i}}{\alpha_{x_i} + \beta_{x_i}}$  ( $x_i = m_i, n_i$ ),  $h_i^\infty = \frac{1}{1 + e^{(V_i + 60)/6.2}}$ . The voltage-dependent rates  $\alpha_{x_i}$  and  $\beta_{x_i}$  ( $x = m, n, h$ ) do depend on temperature as follows:

$$\alpha_{m_i} = \phi(T) \frac{0.182(V_i + 30)}{1 - e^{-(V_i + 30)/8}}, \tag{3a}$$

**Fig. 1** (Color online) **a–b** The sketch of network topologies. **a** A circular network with two nearest neighbors for periodic boundary conditions. **b** The small-world network in which the disconnected edge is randomly rewired with probability  $p$



$$\beta_{n_i} = -\phi(T) \frac{0.124(V_i + 30)}{1 - e^{-(V_i+30)/8}}, \tag{3b}$$

$$\alpha_{n_i} = \phi(T) \frac{0.01(V_i - 30)}{1 - e^{-(V_i-30)/9}}, \tag{3c}$$

$$\beta_{h_i} = -\phi(T) \frac{0.002(V_i - 30)}{1 - e^{-(V_i-30)/9}}, \tag{3d}$$

$$\alpha_{h_i} = \phi(T) \frac{0.028(V_i + 45)}{1 - e^{-(V_i+45)/6}}, \tag{3e}$$

$$\beta_{h_i} = -\phi(T) \frac{0.091(V_i + 70)}{1 - e^{-(V_i+70)/6}}. \tag{3f}$$

where  $\phi(T) = Q_{10}^{\frac{T-23}{10}}$  in which the effect of temperature on gate rates is an exponential function [48].  $Q_{10}$  is the temperature coefficient on gating rates, and  $T$  denotes the temperature expressed in Celsius. The factors  $g_{i,j}$  are given by  $g_{i,j} = 1 (g_{j,i} = 1)$  when the node  $j$  interacts with node  $i$ , and otherwise  $g_{i,j} = 0$ . The degree of the node  $i$  can be computed by  $k_i = \sum_{j=1}^N g_{i,j}$ . In order to build the network, we use the standard algorithm, i.e., we start from a ring with periodic boundary conditions. Let  $g_{N,k}$  ( $N = 200, k = 2$ ) be a  $2k$ -circulant network with vertex set  $V(g_{N,k}) = \{v_1, v_2, \dots, v_n\}$  and edge set  $E(g_{N,k}) = (v_i, v_{i+n}) : 1 \leq i \leq N, 1 \leq n \leq k (i + n \equiv j \pmod{N} \text{ if } i + n > N)$ . Then, we disconnect and reconnect each edge of  $g_{N,k}$  with probability  $p$  by changing uniformly and randomly one end of an edge, and repeat this process for each node as shown in Fig. 1. In this process, loops and multi-edges are not allowed [24]. We chose the neuron with the largest degree as the pacemaker (hub neuron) in the neuronal network, and denote by  $i_0(t)$ , the square wave signal sent to the pacemaker, i.e., we set  $I_{i=d} = 1$ , and

$$i_0(t) = \begin{cases} I_0, & nT' + 0 \leq t < nT' + \frac{T'}{2}, \\ 0, & nT' + \frac{T'}{2} \leq t < nT' + T', \end{cases} \tag{4}$$

where  $n$  is positive integer, and  $I_0$  and  $T'$  stands for the amplitude and period of the square wave signal, respectively. The description and the values of the parameters is given in Table 1.

To quantify transmission of firing in the neuronal network, we calculate the response  $Q_i$ , defined as  $Q_i = |\langle e^{i\omega x_i(t)} \rangle|$  [54], where  $|\cdot|$  and  $\langle \cdot \rangle$  denote module and time average, respectively. The membrane potential  $V_i(t)$  is converted into the pulses series  $x_i = V_A$  with 1ms bin or  $V_B, V_A = 1$  and  $V_A = 0$  corresponding to the firing and nonfiring states, respectively. From the definition of  $Q_i$ , one can find that the value of  $Q_i$  is proportional to the Fourier transform coefficient  $F(\omega')$  at  $\omega' = \omega [F(\omega') = \int_0^{+\infty} e^{i\omega' t} x(t) dt]$ . We argue that calculating  $Q_i$  is faster than obtaining the Fourier transform coefficient. Furthermore, we can get the relationship between  $Q_i$  and the firing rate  $r_i$ , which is defined as the number of spiking at a given time assuming that the spiking of the neuron is periodic.  $Q_i$  may be written as,

$$Q_i = r_i T' \frac{\sqrt{2 - 2 \cos(2\pi/T')}}{\pi}. \tag{5}$$

The factor  $Q_i$  detects the frequency of square wave, and a large  $Q_i$  is observed when synchronization emerges. Signal propagation is achieved when the output firing is synchronized with the stimulating signal. In neuron systems, the stimulus information is transmitted by the firing rate coding mechanism, and we are thus interested in the transmission of firing rate which contains relevant information about the pacemaker.

**Table 1** Parameter values

Parameter	Description	Value
$C_m$	Cell membrane capacitance	0.75 mF/cm <sup>2</sup>
$g_{Na}$	The maximum conductance for sodium	150.0 mS/cm <sup>2</sup>
$g_K$	The maximum conductance for potassium	40.0 mS/cm <sup>2</sup>
$g_l$	The maximum leakage conductance	0.033 mS/cm <sup>2</sup>
$V_K$	The reversal potential for potassium	-90.0 mV
$V_{Na}$	The reversal potential for sodium	60.0 mV
$V_l$	Leakage reversal potential	-70.0 mV
$I_0$	The amplitude of the square wave signal	0.0 40.0 μA/cm <sup>2</sup>
$T'$	The period of the square wave signal	100ms
$\epsilon$	The coupling strength	0.0–5.0 mS/cm <sup>2</sup>
$p$	The connection probability of small-world network	0.0–1.0
$Q_{10}$	The temperature coefficient	2.3 °C
$T$	The Celsius temperature	0–50 °C

### 3 Observations and results

First, we investigate the effect of temperature on the response of small-world neuronal network driven by a pacemaker. We examine the activity in such a network at different temperatures. Figure 2 shows the average response  $Q_{aver} = \frac{1}{N} \sum_{i=1}^N Q_i$  as a function of temperature  $T$  for the different values of the coupling strength. From those curves, one may clearly observe that there is an optimal range of temperature to obtain a large value of  $Q_{aver}$  with different coupling strengths, and the usual resonance clearly emerges. This suggests that temperature is instrumental in achieving effective signal transmission from pacemaker to the whole network.

Figure 3 shows a color 3D plots of  $Q_i$  as a function of  $i$  (index of coupled neurons) and  $T$  for different values of the coupling strength  $\epsilon$ . Looking at the  $i$ -axis, one may see some large value of  $Q_i$  for each neuron, indicating that the signal of pacemaker can be transmitted to the whole network at intermediate temperature irrespective of  $\epsilon$ . Looking at the  $T$ -axis, we see that a maximum of  $Q_i$  exists for an appropriate value of  $T$ , i.e., a resonant behavior exists for pacemaker-driven neurons for all  $\epsilon$ . Interestingly, we find that neurons show no electrical activity except for the hub node at high temperature.

To further assess the temperature role on the transmission of pacemaker signal, Fig. 4a–c presents  $r_i$  ( $i = 1, 2, 5, d, 200$  ( $d = 194$ )) versus  $T$  for with

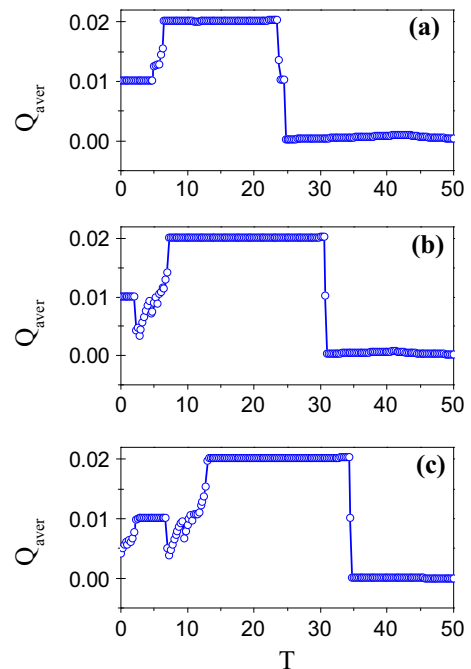


**Fig. 2** (Color online) a–c The average response  $Q_{aver}$  against temperature  $T$  for different coupling strength  $\epsilon = 1.0, 2.0,$  and  $3.0,$  respectively. Here,  $p = 0.3$

$\epsilon = 1.0, 2.0$  and  $3.0,$  respectively. One can see clearly that  $r_i$  increases with  $T$  and then decreases after reaching a maximum. This again indicates a resonant phe-

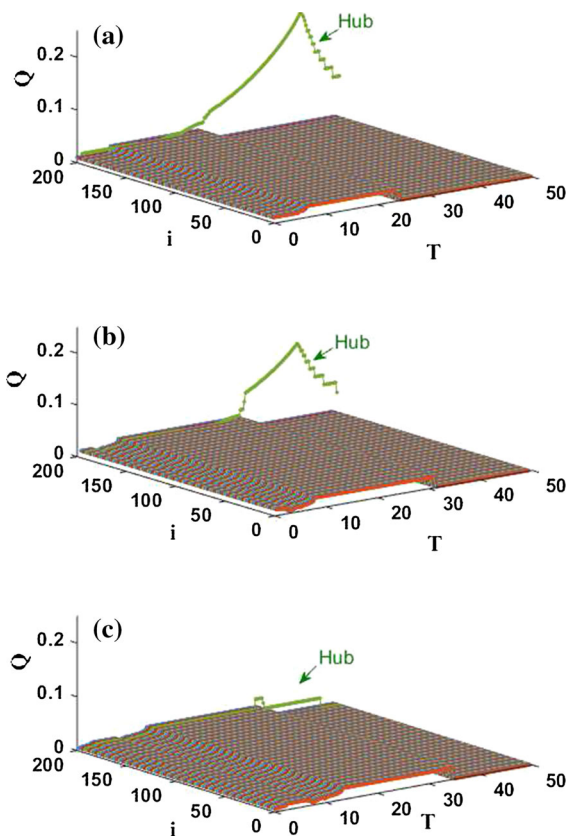


**Fig. 3** (Color online) **a–c** The 3D plot of of the response  $Q$  as a function of  $i$  and  $T$  for  $\epsilon = 1.0, 2.0,$  and  $3.0,$  respectively

nomenon. We also find that  $r_i = 0.01 = \frac{1}{T^r}$  at an optimal window (identified by an arrow), indicating that the whole network is synchronized with the signal of pacemaker. We call it full synchronization window (FS window), which are marked by the arrow in Fig. 4d. Interestingly, one observe  $r_i = \frac{1}{T^r}$  and  $r_d \neq \frac{1}{T^r}$  at another window, indicating that all neurons except for the hub node are entrained by the signal of pacemaker, i.e., remote synchronization occurs. We call it remote synchronization window (RS window). Furthermore, the comparison between numerical results and analytical results (Eq. 5) is shown in Fig. 4d–f. They are in good agreement when the spiking of neuron is periodic. Upon comparing the three subfigures, we find that the width of the optimal window depends nonmonotonically on the coupling strength, which itself critically controls to which extent the network is under the influence of the pacemaker.

In order to gain more insight into the role of temperature on the signal propagation of pacemaker, we turn

to investigate the effect of the others parameters on the temperature-optimized signal propagation. Figure 5a–f gives the dependence of  $r_i$  on the temperature  $T$  for the different connection probability  $p$ . From Fig. 5b–e (the small-world network), we see similar resonances for different connection probabilities, indicating that the phenomenon of temperature-optimized signal propagation is general. We also see that there exist FS and RS windows also for different connection probabilities. For a regular network ( $p = 0.0$ ), however, the firing rate increases with the increase in temperature for a fraction of the neurons, while a similar resonance phenomenon may be also observed in the random network. Interestingly, full and remote synchronization cannot be observed if one take a closer look at the pattern in Fig. 5f.

We now consider the effect of coupling strength  $\epsilon$  on the signal propagation of pacemaker. In Fig. 6, the relationship between  $r_i$  and  $\epsilon$  for different  $T$  is exhibited. One can notice that there exists a window in which all neurons spikes with the same firing rate at low temperature, while they are not entrained by the signal of pacemaker [Fig. 6a]. With the increase in temperature, full synchronization and remote synchronization occur in an optimal windows, and resonance-like behavior may be observed [Fig. 6b, c]. For higher temperature, the firing rate of the hub node vanishes for increasing  $\epsilon$ , and there are not spikes in the whole neuronal network at sufficient large coupling strength [Fig. 6d]. These results suggest that the coupling strength plays a crucial role in the signal transmission of pacemaker.

Figure 7 shows the firing rates  $r_1$  and  $r_{Hub}$  as a function of the coupling  $\epsilon$  for different temperatures. The upper and lower columns in Fig. 7 correspond to  $r_1$  and  $r_{Hub}$ , respectively. The different curves stand for the different reconnection probability in each subfigure. Nonmonotonic curves for  $r_1$  may be observed, indicating that the coupling strength-optimized signal propagation can also be obtained for different reconnection probability, while  $r_{Hub}$  decreases monotonously for increasing  $\epsilon$ . Furthermore, the full and remote synchronization phenomena may also occur at the appropriate temperature [Fig. 7b–c].

In order to appreciate the details of the dynamics, we show [see Fig. 8a–d] the time series for  $x_1, x_4, x_5, x_d$  ( $d = 194$ ), and  $x_{200}$  for  $T = 0.0, 10.0, 20.0$  and  $40.0$ , respectively. Figure 8a shows synchronous spiking, which are not entrained by the signal of pacemaker, and Fig. 8b shows that all neurons spike with

**Fig. 4** (Color online) **a–c** Dependence of the firing rate  $r_i$  ( $i = 1, 2, 5, d, 200$ ) on the temperature  $T$  for  $\epsilon = 1.0, 2.0,$  and  $3.0$ , respectively. The index  $d$  stands for the hub node. **(d)–(f)** The zoomed-in part of **(a)–(c)**, the pink lines stand for the theoretical result from Eq. 5

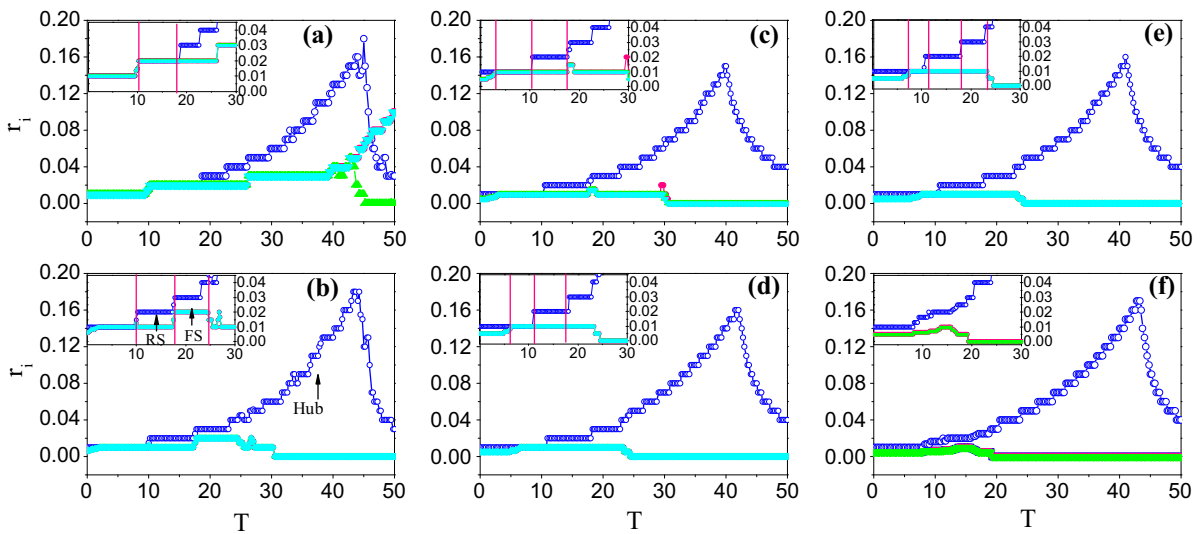
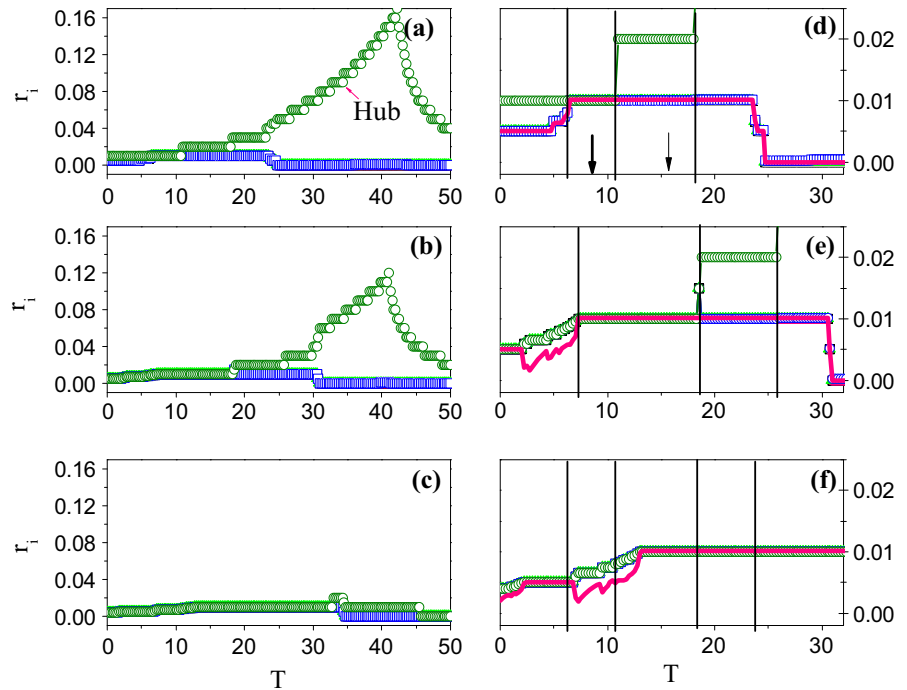


**Fig. 5** (Color online) Plots of the firing rate  $r_i$  ( $i = 1, 2, 5, d, 200$ ) on the temperature  $T$  for the different connection probability of small world network.  $p = 0.0$  (a),  $0.1$  (b),

$0.3$  (c),  $0.5$  (d),  $0.7$  (e), and  $1.0$  (f).  $\epsilon = 1.0$ . The insets show the zoomed-in part. The letters FS and RS stand for the full synchronization and remote synchronization, respectively

the same frequency, which corresponds to driving frequency of the pacemaker, indicating that full synchronization occurs. Figure 8c illustrates a case where we have remote synchronization. Interestingly, in Fig. 8d, one may clearly observe that the hub node spikes with

bursting, while others neurons oscillate with a small amplitude.

To further investigate the change of dynamical behaviors in details, Fig. 9 shows the bifurcation of ISI of membrane potential, which is the interval time of



**Fig. 6** (Color online) **a–d** The firing rate  $r_i$  ( $i = 1, 2, 5, d, 200$ ) ( $d = 194$ ) vs  $\epsilon$  for  $T = 0.0, 10.0, 20.0,$  and  $40.0,$  respectively.  $p = 0.3$

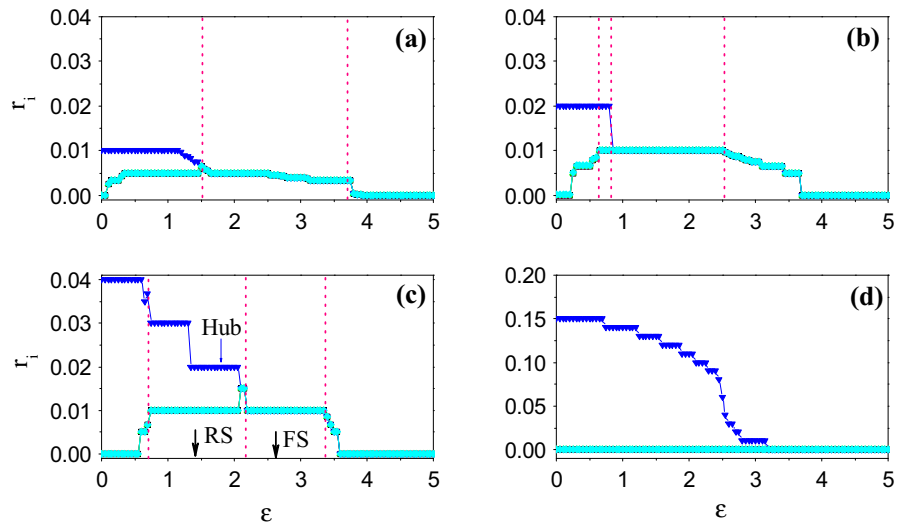
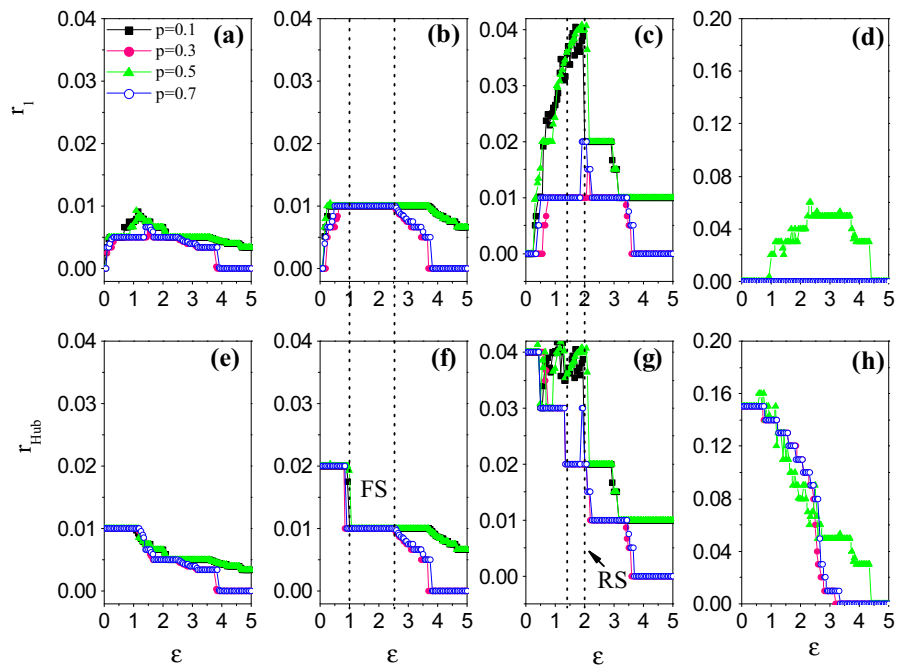


**Fig. 7** (Color online) **a–d** The firing rate  $r_1$  against  $\epsilon$  for  $T = 0.0, 10.0, 20.0,$  and  $40.0,$  respectively, **e–h** the firing rate  $r_{Hub}$  versus  $\epsilon$  for  $T = 0.0, 10.0, 20.0,$  and  $40.0,$  respectively



serial spikes for  $V_1(t)$  (Fig. 9a–c) and  $V_d(t)$  (Fig. 9d–f) with different coupling strength. The left, middle and right columns corresponds to  $\epsilon = 1.0, 2.0,$  and  $3.0,$  respectively. For the different neurons (the hub and other nodes), the membrane potentials show different electrical modes. For other nodes (except for the hub node), it may be clearly observed that neuron frequency is shifted from the periodic spiking with  $\frac{\omega'}{\omega} = 1 : 2$  ( $\omega'$  and  $\omega$  correspond to the frequencies of spiking and pacemaker, respectively) to the periodic spiking corre-

sponding to  $1 : 1$  as the temperature increases [Fig. 9a–c]. However, for the hub node, periodic bursting, periodic spiking and aperiodic bursting can be observed as the temperature increases [Fig. 9d–f]. Interestingly, comparing the corresponding columns in the two sub-figures, one clearly see the FS window for spiking with  $\frac{\omega'}{\omega} = 1 : 1$  and RS window, where the neuron shows periodic spiking, while the hub node shows bursting.

Finally, we report the dynamical phase diagrams in the  $(\epsilon, T)$  plane for the node with index  $i = 1$  (Fig. 10a)

**Fig. 8** (Color online) **a–d** Time series  $x_i(t)$ , ( $i = 1, 2, 5, d, 200$ ) ( $d = 194$ ) for  $T = 0.0, 10.0, 20.0$ , and  $40.0$ , respectively. The green and pink lines stand for the square wave signal and hub node, respectively. Here,  $\epsilon = 2.0$ ,  $p = 0.3$

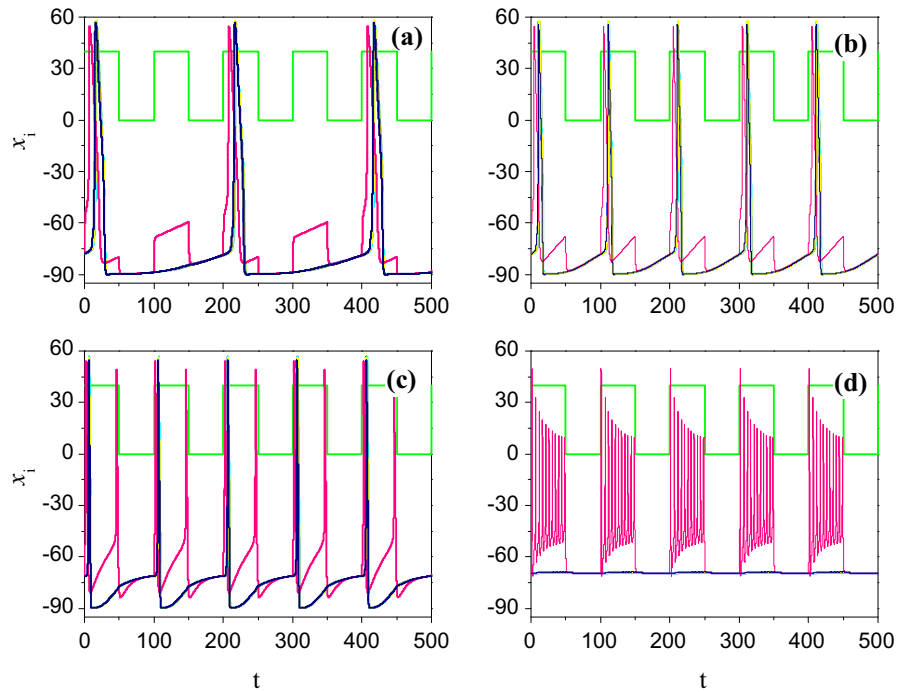
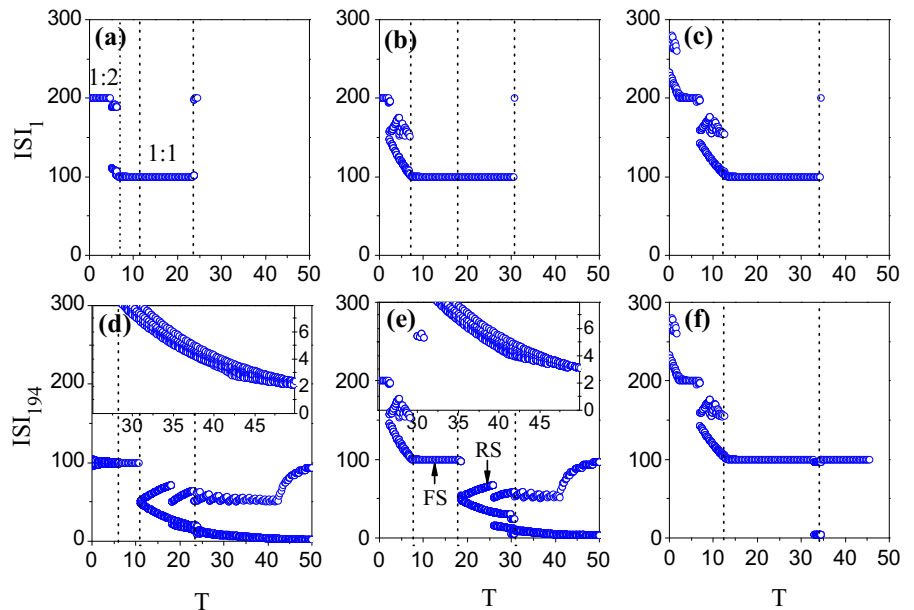


**Fig. 9** (Color online) **a–d** The bifurcation of ISI of membrane potential which is defined by the interval time of spiking. For upper to lower rows,  $V_1(t)$  and  $V_{Hub}(t)$  are chosen. The left, middle and right columns correspond to  $\epsilon = 1.0, 2.0$ , and  $3.0$ , respectively. Here,  $p = 0.3$



and hub node (Fig. 10b). Based on the above observations, we conclude that neurons may exhibit four primary features: subthreshold oscillation state (SO), spiking state with 1 : 1 (SS1), spiking state with 1 : 2 (SS2) and bursting state (BS). In Fig. 10, the yellow region corresponds to BS state, in which neurons show bursting state, the gray region corresponds to SO state,

where the potential  $V(t)$  oscillates around the steady state with a small amplitude, and the SS1 and SS2 states for  $\frac{\omega'}{\omega} = 1 : 1$ , and  $1 : 2$  are marked by pink and cyan, respectively. Comparing Fig. 10a–b, one finds that the pink regions corresponding to the hub and other neurons are different, which leads to FS and RS, and



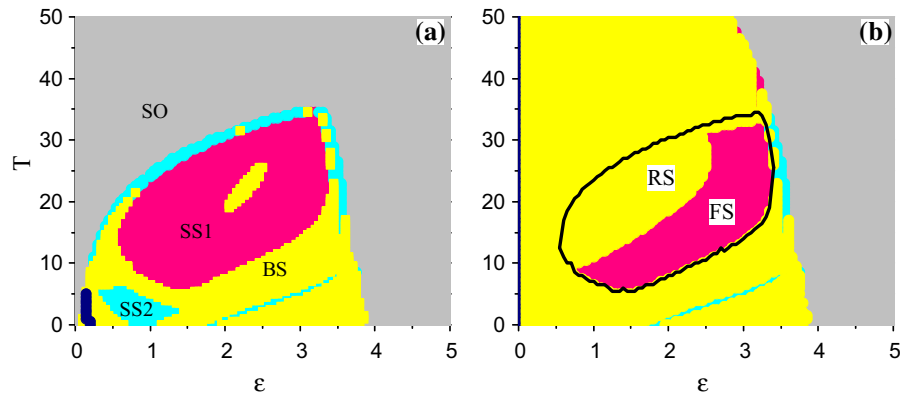


**Fig. 10** (Color online) **a–b** The dynamical phase diagrams for the  $V_1(t)$  and  $V_{Hub}(t)$ , respectively. The pink region corresponds to frequency synchronization with  $\frac{\omega}{\omega'} = 1 : 1$ , where  $\omega$  is the frequency of pacemaker,  $\omega'$  is the frequency of spiking. The letters

SO, SS1, SS2, BS FS and BS stand for the subthreshold oscillation state, spiking state with phase-locking rate 1 : 1, spiking state with phase-locking rate 1 : 2, bursting state full synchronization and remote synchronization, respectively

depends on both  $\epsilon$  and  $T$ , showing an island shape. This result suggests that the signal of pacemaker may propagate effectively only at for an appropriate choice of temperature and coupling strength.

#### 4 Conclusions

In conclusion, we have discussed in detail the transmission of pacemaker signal in small-world neural networks with a biologically plausible neuron model, and where the environmental temperature is a relevant parameter. In our model, one stimulated neuron represents the pacemaker, and we have found that the network synchronizes with the stimulating signal only for an appropriate choice of temperature, indicating that the signal transmission may be optimized. Interestingly, this synchronous behavior may occur in two forms: full synchronization, where all the neurons are entrained by the stimulating signal, and remote synchronization, where all neurons, except for the pacemaker, synchronize with the stimulating signal. Furthermore, a rich variety of dynamical behaviors has been observed, including spiking with rate of phase locking 1 : 1 and 1 : 2, and bursting. We have also found that the phenomenon of temperature-optimized signal transmission is general. In fact, numerical simulations with different values of the coupling strength and the connection probability of the small world network have been systematically per-

formed, and similar results have been observed. Rather surprisingly, we have found that a resonant behavior, in which the response of neuronal network nonmonotonically depends on the coupling strength, may be also observed.

The environmental temperature critically determines whether biological organisms properly work. It is necessary for any biological system to survive in an appropriate temperature range, with higher or lower temperatures that may challenge the normal functioning of organisms. Motivated by the experimental findings about the effect of temperature on the neuronal firing [55,56], we have investigated the effect of temperature on the rhythmic behavior of neuronal networks driven by a pacemaker, which is an important topic in neuroscience. Our findings provide new insights on the subject, and improve our understanding about the existence of the optimal temperature observed in experiments performed with living biological systems.

**Acknowledgements** This work was supported partially by the National Natural Science Foundation of China under Grant Nos. 11675112 and 11805091.

**Data availability** The datasets generated during and/or analyzed during the current study are available from the corresponding author on reasonable request.

**Declarations**

**Conflict of interest** The authors declare that there is no conflict of interest to this work.

## References

1. Marder, E.: Moving rhythms. *Nature* **410**, 755 (2001)
2. Koshiya, N., Smith, J.C.: Neuronal pacemaker for breathing visualized in vitro. *Nature* **400**, 360–363 (1999)
3. Marder, E., Bucher, D.: Central pattern generators and the control of rhythmic movements. *Curr. Biol.* **11**, R986–R996 (2001)
4. Rabbah, P., Nadim, F.: Distinct synaptic dynamics of heterogeneous pacemaker neurons in an oscillatory network. *J. Neurophysiol.* **97**, 2239–2253 (2007)
5. Wang, X.J.: Pacemaker neurons for the theta rhythm and their synchronization in the septohippocampal reciprocal loop. *J. Neurophysiol.* **87**, 889–900 (2002)
6. Gu, H., Ren, W., Lu, Q., Wu, S., Yang, M., Chen, W.: Integer multiple spiking in neuronal pacemakers without external periodic stimulation. *Phys. Lett. A* **285**, 63–68 (2001)
7. Gu, H.G.: Experimental observation of transition from chaotic bursting to chaotic spiking in a neural pacemaker. *Chaos* **23**, 023126 (2013)
8. Eisen, J.S., Marder, E.: Mechanisms underlying pattern generation in lobster stomatogastric ganglion as determined by selective inactivation of identified neurons. III. Synaptic connections of electrically coupled pyloric neurons. *J. Neurophysiol.* **48**, 1392–1415 (1982)
9. Nagai, Y., Gonzalez, H., Shrier, A., Glass, L.: Paroxysmal starting and stopping of circulating waves in excitable media. *Phys. Rev. Lett.* **84**, 4248 (2000)
10. Perc, M., Gosak, M.: Pacemaker-driven stochastic resonance on diffusive and complex networks of bistable oscillators. *New J. Phys.* **10**, 053008 (2008)
11. Perc, M.: Stochastic resonance on excitable small-world networks via a pacemaker. *Phys. Rev. E* **76**, 066203 (2007)
12. Kori, H., Mikhailov, A.S.: Entrainment of randomly coupled oscillator networks by a pacemaker. *Phys. Rev. Lett.* **93**, 254101 (2004)
13. Yao, C.G., Ma, J., Zhiwei He, Z.W., Nakano, T., Qian, Y., Shuai, J.W.: Inhibitory-autapse-enhanced signal transmission in neural networks. *Nonlinear Dyn.* **97**, 1425–1437 (2019)
14. Qin, H., Ma, J., Wang, C., Wu, Y.: Autapse-induced spiral wave in network of neurons under noise. *PLoS One* **9**, e100849 (2014)
15. Ma, J., Tang, J.: A review for dynamics in neuron and neuronal network. *Nonlinear Dyn.* **89**, 1569–1578 (2017)
16. Ma, J., Tang, J.: A review for dynamics of collective behaviors of network of neurons. *Sci. China Technol. Sci.* **58**, 2038–2045 (2015)
17. Jia, Y.B., Gu, H.G., Li, Y.Y., Ding, X.L.: Inhibitory autapses enhance coherence resonance of a neuronal network. *Commun. Nonlinear Sci. Numer. Simul.* **95**, 105643 (2021)
18. Guan, L., Gu, H.G., Zhao, Z.G.: Dynamics of sub-threshold and suprathreshold resonance modulated by hyperpolarization-activated cation current in a bursting neuron. *Nonlinear Dyn.* **104**, 577–601 (2021)
19. Xu, Y., Jia, Y., Wang, H.W., Liu, Y., Wang, P., Zhao, Y.J.: Spiking activities in chain neural network driven by channel noise with field coupling. *Nonlinear Dyn.* **95**, 3237–3247 (2019)
20. He, Z.W., Yao, C.G.: The effect of oxygen concentration on the coupled neurons: rich spiking patterns and synchronization. *Sci. China Technol. Sci.* **63**, 2339–2348 (2020)
21. Yao, Z., Wang, C., Zhou, P., Ma, J.: Regulating synchronous patterns in neurons and networks via field coupling. *Commun. Nonlinear Sci. Numer. Simul.* **95**, 105583 (2021)
22. Lago-Fernandez, L.F., Huerta, R., Corbacho, F., Siguenza, J.A.: Fast response and temporal coherent oscillations in small-world networks. *Phys. Rev. Lett.* **84**, 2758 (2000)
23. White, J.G., Southgate, E., Thompson, J.N., Brenner, S.: The structure of the nervous system of the nematode *Caenorhabditis elegans*. *Phil. Trans. R. Soc. Lond. B* **314**, 1–340 (1986)
24. Watts, D.J., Strogatz, S.H.: Collective dynamics of small-world networks. *Nature* **393**, 440–442 (1998)
25. Liu, Y., Xu, Y., Ma, J.: Synchronization and spatial patterns in a light-dependent neural network. *Commun. Nonlinear Sci. Numer. Simul.* **89**, 105297 (2020)
26. Sun, X.J., Perc, M., Lu, Q.S., Kurths, J.: Effects of correlated Gaussian noise on the mean firing rate and correlations of an electrically coupled neuronal network. *Chaos* **20**, 033116 (2010)
27. Yao, C.G., Zhan, M., Shuai, J.W., Ma, J., Kurths, J.: Insensitivity of synchronization to network structure in chaotic pendulum systems with time-delay coupling. *Chaos* **27**, 126702 (2017)
28. Tang, J., Zhang, J., Ma, J., Luo, J.M.: Noise and delay sustained chimera state in small world neuronal network. *Sci. China Technol. Sci.* **62**, 1134–1140 (2019)
29. Xu, Y., Jia, Y., Ge, M.Y., Lu, L.L., Yang, L.J., Zhan, X.: Effects of ion channel blocks on electrical activity of stochastic Hodgkin-Huxley neural network under electromagnetic induction. *Neurocomputing* **283**, 196–204 (2017)
30. Ozer, M., Uzuntarla, M., Kayikcioglu, T., Graham, L.J.: Collective temporal coherence for subthreshold signal encoding on a stochastic small-world Hodgkin-Huxley neuronal network. *Phys. Lett. A* **372**, 6498–6503 (2008)
31. Jun, M., Yang, L.J., Wang, Y., Zhang, C.R.: Spiral wave in small-world networks of Hodgkin-Huxley neurons. *Commun. Theor. Phys.* **54**, 583–588 (2010)
32. Lv, M., Ma, J., Yao, Y.G., Alzahrani, F.: Synchronization and wave propagation in neuronal network under field coupling. *Sci. China Technol. Sci.* **62**, 448–457 (2019)
33. Qian, Y., Zhang, C., Wei, Z.G., Liu, F., Yao, C.G., Zheng, Z.G.: The optimal oscillation mode in excitable small-world networks. *Europhys. Lett.* **131**, 38002 (2020)
34. Bazhenov, M., Timofeev, I., Steriade, M., Sejnowski, T.J.: Potassium model for slow (2–3 Hz) in vivo neocortical paroxysmal oscillations. *J. Neurophysiol.* **92**, 1116–1132 (2004)
35. Wu, X.X., Shuai, J.W.: Multistability in a neuron model with extracellular potassium dynamics. *Phys. Rev. E* **85**, 061911 (2012)
36. Wu, X.X., Shuai, J.W.: Effects of extracellular potassium diffusion on electrically coupled neuron networks. *Phys. Rev. E* **91**, 022701 (2015)
37. Wu, X.X., Yao, C.G., Shuai, J.W.: Enhanced multiple vibrational resonances by Na<sup>+</sup> and K<sup>+</sup> dynamics in a neuron model. *Sci. Rep.* **5**, 7684 (2015)
38. Shuai, J.W., Sheng, R., Jung, P.: Entropically modified spiking ability and periodicity in clustered channels. *Phys. Rev. E* **81**, 051913 (2010)

39. Shuai, J.W., Bikson, M., Hahn, P.J., Lian, J., Durand, D.M.: Ionic mechanisms underlying spontaneous CA1 neuronal firing in  $\text{Ca}^{2+}$ -free solution. *Biophys. J.* **84**, 2099–2111 (2003)
40. Roper, S.N., Obenaus, A., Dudek, F.E.: Osmolality and non-synaptic epileptiform bursts in rat CA1 and dentate gyrus. *Ann. Neurol.* **31**, 81–85 (1992)
41. Snow, R.W., Dudek, F.E.: Electrical fields directly contribute to action potential synchronization during convulsant-induced epileptiform bursts. *Brain Res.* **323**, 114–118 (1984)
42. Wei, Y., Ullah, G., Schiff, S.J.: Unification of neuronal spikes, seizures, and spreading depression. *J. Neurosci.* **34**, 11733–11743 (2014)
43. Ullah, G., Wei, Y., Dahlem, M.A., Wechselberger, M., Schiff, S.J.: The role of cell volume in the dynamics of seizure, spreading depression, and anoxic depolarization. *PLoS Comput. Biol.* **14**, 1004414 (2015)
44. Yao, C.G., He, Z.W., Nakano, T., Shuai, J.W.: Spiking patterns of a neuron model to stimulus: Rich dynamics and oxygens role. *Chaos* **28**, 083112 (2018)
45. Somero, G.N.: Temperature adaptation of enzymes: biological optimization through structure-function compromises. *Ann. Rev. Ecol. Syst.* **9**, 1–29 (1978)
46. Temperature effects on biological systems: rowbury. *Introduction. Sci. Prog.* **86**, 1–8 (2003)
47. Schipper, L.A.: On the temperature dependence of enzymecatalyzed rates. *Biochemistry* **55**, 1681–1688 (2016)
48. Song, X.L., Wang, H.T., Chen, Y., Lai, Y.C.: Emergence of an optimal temperature in action-potential propagation through myelinated axons. *Phys. Rev. E* **100**, 032416 (2019)
49. Fu, X., Yu, Y.G.: Reliable and efficient processing of sensory information at body temperature by rodent cortical neurons. *Nonlinear Dyn.* **98**, 215–231 (2019)
50. Yu, Y.G., Shu, Y.S., McCormick, D.A.: Cortical action potential backpropagation explains spike threshold variability and rapid-onset kinetics. *J. Neurosci.* **28**, 7260–7272 (2008)
51. Yu, Y.G., Hill, A.P., McCormick, D.A.: Warm body temperature facilitates energy efficient cortical action potentials. *PLoS Comput. Biol.* **8**, 1002456 (2012)
52. Tai, C., Wang, J., Roppolo, J.R., Groat, W.C.: Relationship between temperature and stimulation frequency in conduction block of amphibian myelinated axon. *J. Comput. Neurosci.* **26**, 331–338 (2008)
53. Ding, Q.M., Jia, Y.: Effects of temperature and ion channel blocks on propagation of action potential in myelinated axons. *Chaos* **31**, 053102 (2021)
54. Yao, C.G., He, Z.W.: Anormal diffusion enhancement of resonant responses for coupled oscillator networks to weak signals. *Chaos* **30**, 083120 (2020)
55. Peterson, M.E., Daniel, R.M., Danson, M.J., Eisenthal, R.: The dependence of enzyme activity on temperature: determination and validation of parameters. *Biochem. J.* **402**, 331–337 (2007)
56. Dell, A.I., Pawar, S., Savage, V.M.: Systematic variation in the temperature dependence of physiological and ecological traits. *Proc. Natl. Acad. Sci. U.S.A.* **108**, 10591–10596 (2011)

**Publisher's Note** Springer Nature remains neutral with regard to jurisdictional claims in published maps and institutional affiliations.